ANNALES
UNIVERSITATIS MARIAE CURIE-SKŁODOWSKA
LUBLIN – POLONIA

VOL. LX, 5 SECTIO AA 2005

Nitrogen and argon adsorption on non-graphitized carbon black: Application of Density Functional Theory*

E. A. Ustinov[1], D. D. Do[2]
[1]*On leave from Saint Petersburg State Technological Institute (Technical University), 26 Moskovsky Prospect, 198013, Russia*
[2]*(corresponding author), Department of Chemical Engineering, University of Queensland, St. Lucia, Queensland 4072, Australia*

Analysis of adsorption equilibria of nitrogen at 77 K and argon at 77 and 87.3 K on non-graphitized carbon black (NGCB) is considered with a Non-Local Density Functional Theory (NLDFT). It was shown that nitrogen and argon adsorption isotherms could be quantitatively correlated with a version of NLDFT accounting for the amorphous nature of NGCB and its surface roughness. Instead of being calculated from some standard equations, such as the 10-4-3 Steele equation, the solid-fluid potential is obtained experimentally from adsorption isotherms and it was found to be a fast decaying function that becomes negligibly small at a distance of about two collision diameters from the surface. The model presented in this paper implicitly accounts for the energetic heterogeneity of the disordered graphite surface and yet it retains the simplicity of the conventional NLDFT as applied to graphitized thermal carbon black. The approach may be further extended to slit pores whose walls are non-graphitized surface, and such an approach will raise questions on the conventional approach where pore walls are assumed to behave like a graphite surface.

1. INTRODUCTION

Vast majority of theoretical models developed for characterization of porous materials rely on a reference system, which is supposed to have a similar surface structure as that of pore walls. The simplest and still popular Barrett, Joyner and

* This paper is to honor Professor M. Jaroniec on the occasion of his receiving the Honorary Professorship title at the Maria Curie-Sklodowska University.

Halenda (BJH) method [1] uses the modified Kelvin equation, which accounts for the statistical adsorbed film thickness *t*. This thickness is determined from the reference adsorption isotherm (*t*-curve) on nonporous solid at a given reduced pressure. In the case of siliceous adsorbents such as MCM-41 and SBA-15 having highly ordered mesoporous structure, the BJH method was substantially improved in recent works of Kruk, Jaroniek and Sayari (KJS) [2-4]. The authors introduced a correction to the pore radius, which brought the pore diameter estimation to correspond with that obtained from the X-ray diffraction (XRD) technique. The KJS method of pore size distribution analysis (PSD) was proved to be in excellent agreement with that provided by non-local density functional theory (NLDFT) [5-7]. However, more thermodynamically correct theory based on a reference system was advanced by Derjaguin [8] and Broekhoff and de Boer (DBdB) [9-10]. In spite of their basis in rigorous thermodynamics, the DBdB theory has received less popularity than the BJH and BJH-KJS approaches due to its higher complexity and some disagreement with the XRD estimations of the pore sizes. Ravikovitch and Neimark showed that pore sizes determined with the DBdB theory and NLDFT are only close to each other for pore diameter larger than 7 nm [11]. Further analysis has shown that the discrepancy between the DBdB theory and NLDFT was mainly caused by the assumption that the solid-fluid potential exerted by the cylindrical pore wall is the same as that of a reference flat surface at the same distance. A successful attempt to overcome this drawback was made recently by introducing a curvature-dependent solid-fluid potential to the original DBdB theory [7]. The modified theory (coined as CDP-BdB) was proved to produce the same PSD function for pore sizes larger than 2 nm. As a reference system in that approach we used argon and nitrogen adsorption isotherms on nonporous silica [4, 12]. We have successfully increased the range of applicability of the thermodynamic model.

In the case of carbonaceous materials the PSD analysis has a large degree of uncertainty due to their complex topology and most importantly the absence of reliable independent methods of assessment of pore sizes. As a rule, the pore volume of activated carbons includes micro-, meso-, and macropores, which hampers the application of any continuum models to derive the PSD function. For this reason, in the modern methods of characterization of pore structures it is customary to rely on molecular approaches such as the density functional theory [13-16]. Like the continuum approaches, NLDFT also needs a reference system to determine the solid-fluid molecular parameters, and the graphitized thermal carbon black (GTCB) is commonly used as such a reference solid. However, there were two problems associated with this choice of reference system and they apparently did not attract enough attention. First, the correlation of experimental nitrogen and argon adsorption isotherms on graphitized carbon

black was only qualitative, which decreases the reliability of the PSD analysis in itself. Secondly, it is unlikely that the pore wall surface of activated carbons has the same perfect structure as that of GTCB. Instead we will argue that non-graphitized carbon black (NGCB) has to be considered as a reference system. However, the surface of non-graphitized carbon black is highly heterogeneous [17-21], which does not allow us to rely on the same model for the solid-fluid potential (like the Steele 10-4-3 equation [22]) that is used in NLDFT for the case of GTCB. This situation is similar to that in the case of nitrogen and argon adsorption on silica surface. The NLDFT leads to poor correlation of nitrogen and argon adsorption isotherms on nonporous silica if the 10-4 Lennard–Jones (LJ) equation is taken to account for the interaction between adsorbed molecules and the surface oxygen atoms [11, 22-23]. The reason of the disagreement between the NLDFT predicted isotherm and the experimental data is the amorphous nature of the silica surface. Interestingly, even accounting for the energetic heterogeneity in the framework of patch-wise model did not eliminate the discrepancy completely [24]. Recently we advanced a new way of application of NLDFT to amorphous solids [6-7, 24], and this has allowed us to describe experimental adsorption isotherms quantitatively. The aim of the present paper is to apply this new method to adsorption of nitrogen and argon on non-graphitized carbon black. The implication is that this methodology can be further extended to the PSD analysis of activated carbons on more rigorous basis compared to that using GTCB as a reference system.

2. MODEL

In this work we rely on Tarazona version of non-local density functional theory [25, 26]. The density profile of a fluid close to a solid surface or confined in the pore at equilibrium condition meets the requirement of minimum grand thermodynamic potential:

$$\Omega = \int \rho[f(\mathbf{r},\rho,\overline{\rho}) + u^{ext}(\mathbf{r}) - \mu]d\mathbf{r} \tag{1}$$

where $\rho, \overline{\rho}$ are the local and smoothed fluid densities, respectively; f is the molar Helmholtz free energy; $u^{ext}(\mathbf{r})$ is external potential exerted by the solid; μ is the chemical potential. The molar Helmholtz free energy is represented as a sum of the ideal and excess terms, and the intermolecular interaction potential u:

$$f(\mathbf{r},\rho,\overline{\rho}) = kT[\ln(\Lambda^3\rho) - 1] + f_{ex}(\overline{\rho}) + u(\mathbf{r}) \tag{2}$$

Here k is the Boltzmann constant and Λ is the de Broglie wavelength. The excess free energy is a function of the smoothed density defined as [25, 26]

$$\overline{\rho}(\mathbf{r}) = \int \rho(\mathbf{r}')\omega(|\mathbf{r}-\mathbf{r}'|, \overline{\rho}(\mathbf{r}))d\mathbf{r}' \tag{3}$$

The weighting functional $\omega(|\mathbf{r}-\mathbf{r}'|, \overline{\rho}(\mathbf{r}))$ is chosen in quadratic form of smoothed density to reproduce the hard sphere direct correlation function [26]:

$$\overline{\rho}(\mathbf{r}) = \overline{\rho}_0(\mathbf{r}) + \overline{\rho}_1(\mathbf{r})\overline{\rho}(\mathbf{r}) + \overline{\rho}_2(\mathbf{r})(\overline{\rho}(\mathbf{r}))^2 \tag{4}$$

where $\overline{\rho}_i(\mathbf{r}) = \int \rho(\mathbf{r}')\omega_i(|\mathbf{r}-\mathbf{r}'|)d\mathbf{r}'$ for i = 0, 1, 2. The weight functions $\omega_0(r)$, $\omega_1(r)$, and $\omega_2(r)$ are defined as functions of the distance r from a given point in the region of two collision diameters σ_{ff} [26].

The excess free energy is defined for a reference hard-sphere fluid by the Carnahan – Starling equation [27] as a function of the smoothed density:

$$f_{ex}(\overline{\rho}) = kT\frac{4\overline{\eta}-3\overline{\eta}^2}{(1-\overline{\eta})^2}, \qquad \overline{\eta} = \frac{\pi}{6}d_{HS}^3\overline{\rho} \tag{5}$$

where d_{HS} is the equivalent hard sphere diameter. The contribution of the excess free energy term increases with the increase of the dimensionless density $\overline{\eta}$ and becomes infinite if $\overline{\eta}$ is unity. Qualitatively the situation is the same as that in the case of the van der Waals (VdW) equation: the excess Helmholtz free energy (as well as the pressure) is infinite when the molar volume of the fluid approaches the VdW constant b.

The term for the intermolecular (attractive) interaction potential u is usually defined in the framework of mean field approximation:

$$u(\mathbf{r}) = \frac{1}{2}\int \rho(\mathbf{r}')\phi_{ff}(|\mathbf{r}-\mathbf{r}'|)d\mathbf{r}' \tag{6}$$

where ϕ_{ff} is the interaction potential of two molecules separated by a distance r. The widely used form for the potential ϕ_{ff} is given by the Weeks, Chandler and Andersen (WCA) perturbation scheme [28]:

$$\phi_{ff}(r) = \begin{cases} -\varepsilon_{ff}, & r < r_m \\ 4\varepsilon_{ff}[(\sigma_{ff}/r)^{12} - (\sigma_{ff}/r)^{6}], & r_m < r < r_c \\ 0, & r > r_c \end{cases} \tag{7}$$

Here ε_{ff} is the potential well depth; σ_{ff} is the collision diameter; $r_m = 2^{1/6}\,\sigma_{ff}$ is the distance at which the potential is minimum; r_c is the cutoff distance.

The solid-fluid potential in the case of adsorption on GTCB is usually defined in the form of the Steele equation [29]:

$$u^{ext}(z) = 2\pi\rho_s\varepsilon_{sf}\sigma_{sf}^2\Delta\left[\frac{2}{5}\frac{\sigma_{sf}^{10}}{z^{10}} - \frac{\sigma_{sf}^4}{z^4} - \frac{\sigma_{sf}^4}{3\Delta(0.61\Delta + z)^3}\right] \tag{8}$$

where z is the distance of the molecule from the graphite surface, ρ_s is the graphite density (114 nm^{-3}), ε_{sf} and σ_{sf} are the solid-fluid LJ pairwise parameters, Δ is the graphite layer spacing (0.335 nm).

The requirement of minimum of the grand thermodynamic potential Ω is satisfied if its derivative with respect to density is equal to zero, which leads to the following equation:

$$\begin{aligned} \mu = kT\ln[\Lambda^3\rho(\mathbf{r})] + f_{ex}[\overline{\rho}(\mathbf{r})] + \int \rho(\mathbf{r}')f_{ex}'[\overline{\rho}(\mathbf{r}')]\xi(|\mathbf{r}-\mathbf{r}'|,\mathbf{r}',\overline{\rho}(\mathbf{r}'))d\mathbf{r}' \\ + \int \rho(\mathbf{r}')\phi_{ff}(|\mathbf{r}-\mathbf{r}'|)d\mathbf{r}' + u^{ext}(\mathbf{r}) \end{aligned} \tag{9}$$

where

$$\xi(|\mathbf{r}-\mathbf{r}'|,\mathbf{r}',\overline{\rho}(\mathbf{r}')) = \frac{\omega_0(|\mathbf{r}-\mathbf{r}'|) + \omega_1(|\mathbf{r}-\mathbf{r}'|)\overline{\rho}(\mathbf{r}') + \omega_2(|\mathbf{r}-\mathbf{r}'|)\overline{\rho}^2(\mathbf{r}')}{1 - \overline{\rho}_1(\mathbf{r}') - 2\overline{\rho}_2(\mathbf{r}')\overline{\rho}(\mathbf{r}')} \tag{10}$$

At a given relative bulk pressure p/p_0 the RHS of the above equation is invariant to coordinate **r**, which is possible only when the density has a specified profile. This density profile may be determined by an iterative procedure. Once the density distribution is determined, the amount adsorbed can be calculated by integration of the density over the corresponding volume. In doing so one can determine the amount adsorbed as a function of the bulk pressure at a specified temperature. The chemical potential at a given relative pressure can be

determined with the same model assuming that the fluid is homogeneous and the solid-fluid potential $u^{ext}(\mathbf{r})$ is zero. In this case eq. (9) is reduced to

$$\mu = kT\ln[\Lambda^3\rho] + f_{ex}(\rho) + \rho f'_{ex}(\rho) + (32\sqrt{2}/9)\pi\varepsilon_{ff}\sigma_{ff}^3\rho \tag{11}$$

The bulk pressure can also be determined from NLDFT for the homogeneous fluid and is expressed as follows:

$$p = kT\rho + \rho^2 f'_{ex}(\rho) + (16\sqrt{2}/9)\pi\varepsilon_{ff}\sigma_{ff}^3\rho^2 \tag{12}$$

For simplicity we drop small terms in eqs. (11), (12) associated with the cutoff distance. Bulk density can be determined by the equation of state (12) at a given pressure. Subsequent substitution of the bulk density to eq. (12) determines the chemical potential and then the corresponding density profile by eq. (10).

2.1. Extension of NLDFT to amorphous solids

Poor correlation of adsorption isotherms on amorphous solids like silica with the conventional NLDFT suggests that there should be an alternative way of application of NLDFT to non-crystalline surfaces. In our previous work [6] we showed that even accounting for the energetic heterogeneity in the framework of patch-wise model does not substantially improve the description of experimental nitrogen and argon adsorption isotherm on nonporous silica at their boiling points in the region of multilayer coverage. The reason of falling to correlate the adsorption isotherms by NLDFT was supposed to be a consequence of applying unrealistic solid-fluid potential defined as 10-4 or 9-3 LJ potential to disordered surface structure. Indeed, the 10-4 or 9-3 equation is the result of integration of the LJ pairwise potential over the surface or solid volume with the implicit assumption that centers of surface atoms are located at a plane without any dispersion. To circumvent this difficulty we endeavored to consider both fluid-fluid and solid-fluid interactions in the same framework adopted in NLDFT. In doing so, we suggested that the excess free energy at a position close to the surface does not only depend on the fluid density at that point but also on the concentration of solid in the neighborhood. It means that if the molecule is very close to the solid surface, the effective smoothed density increases due to the contribution of the solid atoms, leading to the increase of the excess free energy. Quantitatively it may be easily accounted for by replacement of the smoothed density with the smoothed void volume $\overline{v} = 1 - \overline{\eta}$. By adding molecules into the void would result in an increase in pressure, which then leads

to an increase in the excess free energy. The essential point is that the excess free energy increases regardless of the course of the decrease in the void volume. The contribution of the solid atoms to the increase of the excess free energy reflects the repulsive forces between the solid and the fluid. Thus, the Carnahan–Starling equation (6) can be rewritten in the following equivalent form:

$$f_{ex}(\bar{v}) = kT(\bar{v}^{-2} + 2\bar{v}^{-1} - 3), \qquad \bar{v} = 1 - \bar{\rho}/\rho_m \tag{13}$$

where $\rho_m = 6/(\pi d_{HS}^3)$ is the maximal fluid density possible, corresponding to $\bar{\eta} = 1$. Equation (4) can now be rearranged in terms of smoothed void volume as follows:

$$\bar{v}(\mathbf{r}) = \bar{v}_0(\mathbf{r}) + \rho_m \bar{v}_1(\mathbf{r})[1 - \bar{v}(\mathbf{r})] + \rho_m^2 \bar{v}_2(\mathbf{r})[1 - \bar{v}(\mathbf{r})]^2 \tag{14}$$

where $\bar{v}_i(\mathbf{r}) = \int v(\mathbf{r}')\omega_i(|\mathbf{r} - \mathbf{r}'|)d\mathbf{r}'$ for i = 0, 1, 2. Here $v(\mathbf{r})$ is the local void volume. The system of equations (13)-(14) is exactly equivalent to eqs. (3)-(4) used in the conventional NLDFT for modeling of homogeneous and inhomogeneous fluids away from the surface where $v(\mathbf{r}) = 1 - \rho/\rho_m$. The difference arises when the position of the fluid molecule is at a distance less than two collision diameters from the surface. In our previous works [6, 7, 24] we assumed that the local void volume is zero everywhere inside the solid and $1 - \rho/\rho_m$ outside the solid, with the solid-fluid interface being of zero thickness. In the present work we will relax this simplification.

To account for a transition zone between the solid and the fluid, we assume that in the absence of fluid molecules the void volume varies in the vicinity of the amorphous solid surface in accordance with the error function:

$$v_s(z) = \frac{1}{\sqrt{2\pi\delta}} \int_{-\infty}^{z} \exp\left[-z^2/(2\delta^2)\right] dz \tag{15}$$

Here δ is the variance, which is a measure of the transition zone thickness. The void volume is zero in the solid and unity in the fluid far away from the surface situated at $z = 0$. In the presence of fluid near the surface the local void volume is

$$v(z) = v_s(z) - \rho(z)/\rho_m \tag{16}$$

Having set the void volume in the vicinity of the solid surface, the smoothed void volume and, consequently, the excess free energy can be found by eqs. (13)-(16).

The described above scheme allows accounting for the repulsive potential arising between the solid and the fluid due to the decrease of the available volume for the fluid molecules because of the appearance of the solid atoms in the proximity of the surface. Following the main idea of the NLDFT of splitting the intermolecular interaction potential into repulsive and attraction terms, one can apply the same scheme to the solid-fluid interaction. In our previous studies we used the WCA perturbation scheme for description of the attractive term of the solid-fluid potential. In that case the solid-fluid collision diameter and the potential well depth were determined by least square fitting. In the present work the solid-fluid attractive potential will be determined directly from the experimental adsorption isotherm using the Tikhonov regularization function [30, 31]. The advantage of such formulation of the task is that we do not impose any definite form of the solid-fluid potential to the system beforehand. Instead we determine this potential from experimental data, which gives important information on the interaction of a fluid molecule with the solid atom.

3. RESULTS AND DISCUSSION

We analyzed nitrogen and argon adsorption isotherms on non-graphitized carbon black Cabot BP 280 [18, 21]. This sample is recommended to be used as a reference solid for characterization of activated carbons instead of GTCB [21].

Nitrogen at 77 K and argon at 87.3 K adsorption isotherms on the sample BP 280 are presented in Figures 1 and 2 in logarithmic and linear scales, respectively. Solid lines are the correlation achieved with the present approach. The fluid-fluid molecular parameters were taken from the paper of Neimark et al. [32].

As is seen from figures, the correlation of the data with the new approach is excellent. For comparison dashed lines in figures are plotted with the conventional NLDFT using the solid-fluid potential well depth ε_{sf}/k of 56.1 K for nitrogen and 58.01 K for argon. These values were obtained for graphitized carbon black. The divergence between the dashed lines and experimental isotherms is very large especially in logarithmic scale, which clearly indicates that the conventional approach is inapplicable to amorphous solids. It should be noted that such good result obtained with our new approach cannot be achieved with the conventional NLDFT even accounting for the energetic heterogeneity in the framework of patch-wise model. It is also not possible to match theoretical and experimental isotherms with the conventional NLDFT by adjusting the solid-fluid potential.

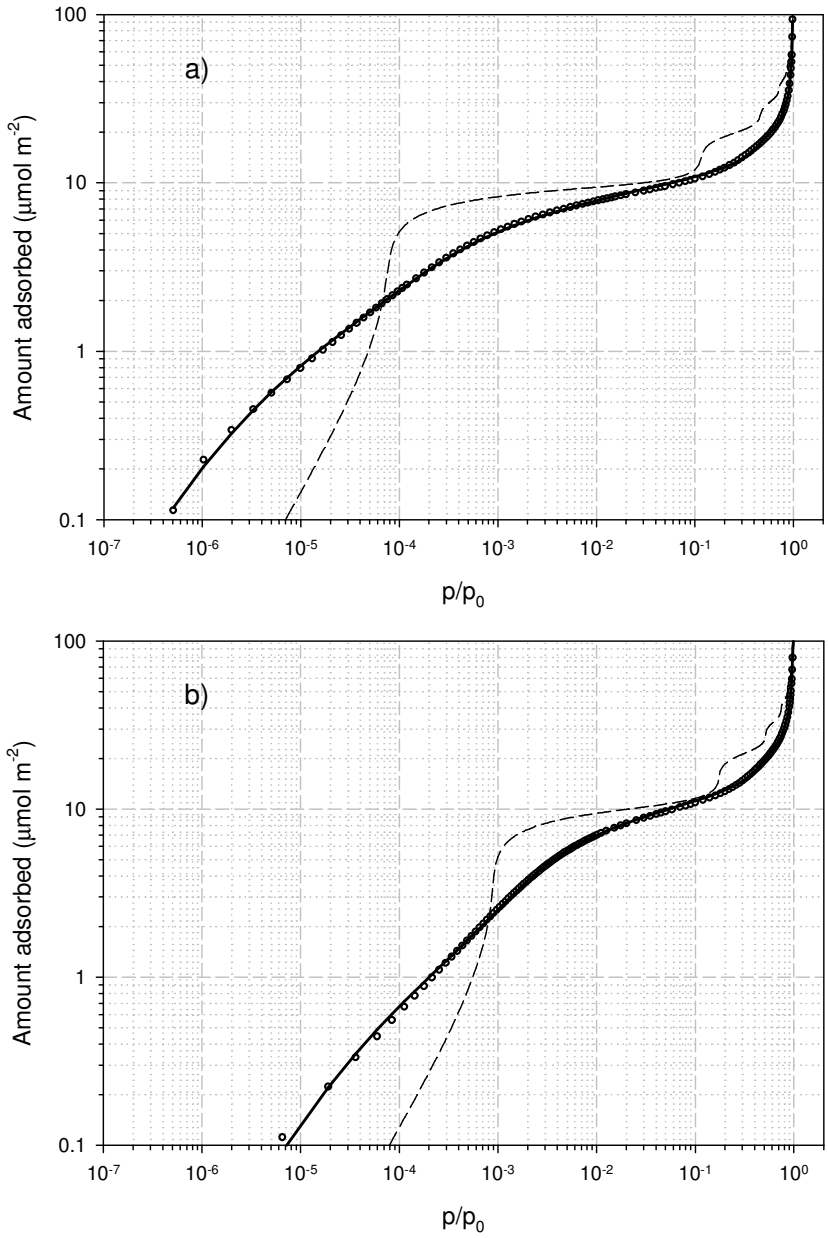

Fig. 1. Nitrogen (a) and argon (b) adsorption isotherms on non-graphitized carbon black Cabot BP 280 [18, 21] at 77 and 87.3 K, respectively in logarithmic scale. (Circles) experimental points, (solid line) correlation with NLDFT adjusted for adsorption on amorphous surface. Dashed line is plotted with the conventional NLDFT for the solid-fluid molecular parameters adjusted to GTCB.

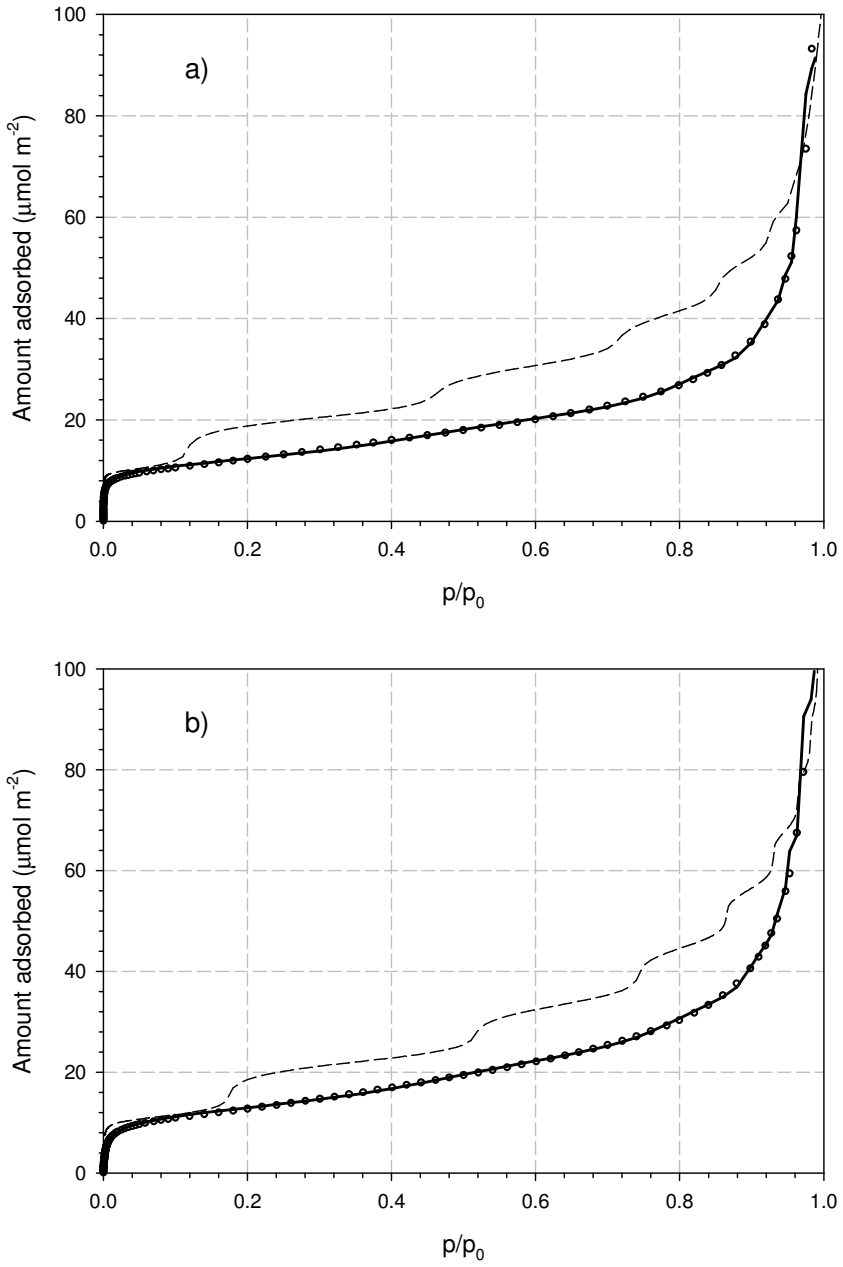

Fig. 2. Nitrogen (a) and argon (b) adsorption isotherms on non-graphitized carbon black Cabot BP 280 in linear scale. Notations are the same as those for Figure 1.

This is because of sharp densification of the adsorbed fluid in the first molecular layer just before its completion resulting in the appearance of an artificial hump on the isotherm. The latter is a consequence of strong fluid-fluid interactions no matter what external potential is imposed on the fluid. There are two ways to suppress the hump. The first one is the decrease of the fluid-fluid interactions in the proximity of the surface, which could be done anyhow, for example, by introducing a non-additivity (damping) factor [33] or an empirical distance-dependent decaying function for the fluid-fluid potential well depth [34]. The second way is the density-dependent repulsive solid-fluid potential, which is realized in our approach.

Figure 3 presents the solid-fluid potential for nitrogen and argon determined with the NLDFT under consideration. Dashed line shows the change of the relative solid density near the solid surface. This curve was calculated at the variation $\delta = 0.1$ nm and its first central moment is placed at the coordinate $z = 0$. To the left of this boundary the relative solid density tends to unity. Line 1 reflects the repulsive potential determined for the limiting case of zero loading.

Note that in the framework of our model the repulsive term of the solid-fluid potential depends on the amount adsorbed because the excess Helmholtz free energy (which is responsible to the repulsive forces) is a function both of the distance from the surface and the density distribution near the solid-fluid interface. The curve 2 shows the variation of the attractive term of the solid-fluid potential, which was determined by the least square procedure. The resulting potential is shown by curve 3. For comparison we also present the Steele potential (dash-dotted lines) derived for the basal graphite plane. Both form and position of the potentials are substantially different. The position at which the potential is minimum for the case of crystalline surface is at about one fluid collision diameter. Fluid molecules cannot approach directly to the surface due to strong repulsive forces. In the case of amorphous surface of non-graphitized carbon black the potential minimum is located on the surface.

It simply means that adsorbed molecules could adsorb on the amorphous surface in gaps between carbon atoms, which could be identified as active sites. Another important feature of the determined potential is that it becomes negligible at a distance larger than about two collision diameters. At present there is not enough information on the exact form of the solid-fluid and the fluid-fluid interactions to explain this experimental result. However, at the present stage this potential can be used in the prediction of the adsorption in slit pores.

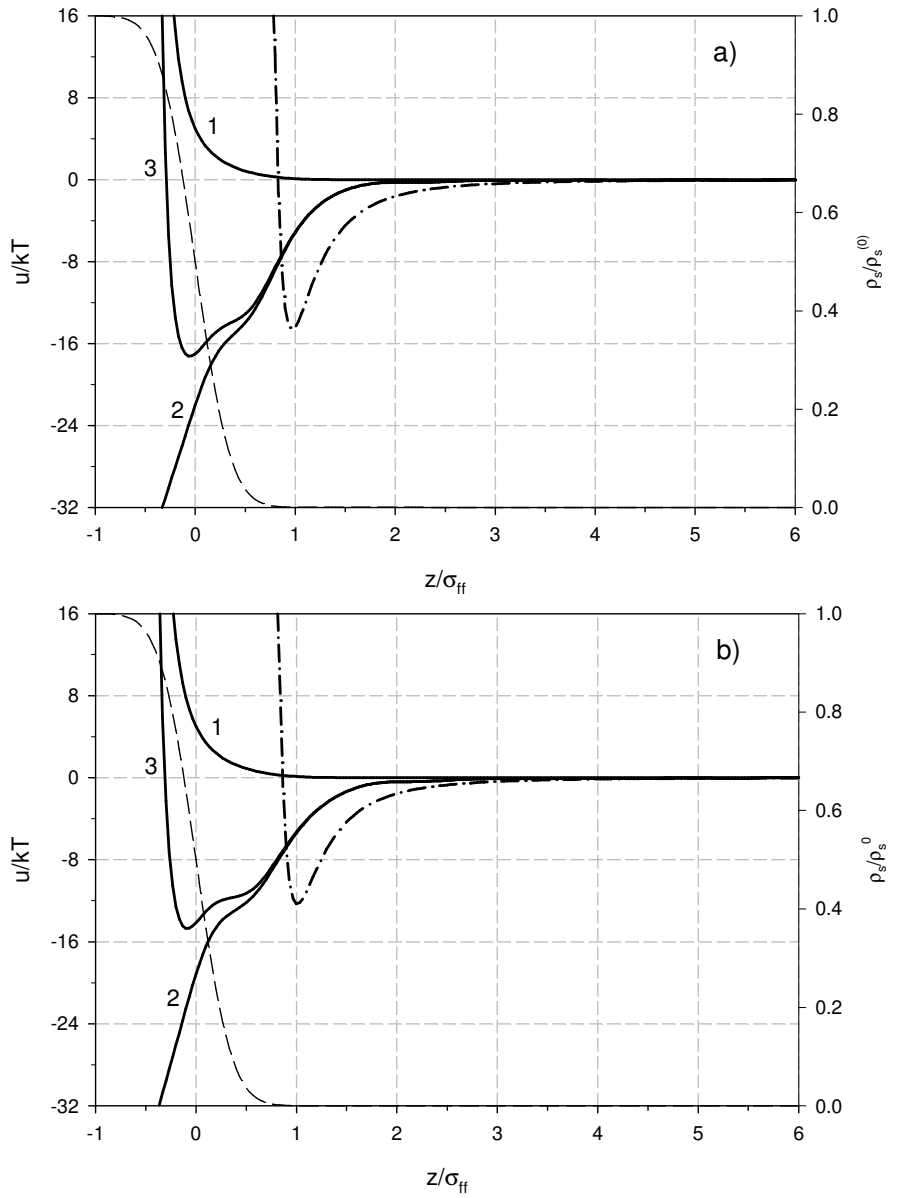

Fig. 3. Solid-fluid potential in the case of N_2 (a) and Ar (b) adsorption on NGCG Cabot BP 280 [18, 21]. (1) repulsive term of the potential numerically equaled to the excess Helmholtz free energy at zero limit of the amount adsorbed; (2) attractive term determined from experimental adsorption isotherms by least square fitting; (3) resulting solid-fluid potential. Dash-dotted line shows the potential exerted by the crystalline surface of GTCB. Dashed line shows the change of the solid density in the vicinity of the surface (see details in the text).

4. CONCLUSIONS

We showed that non-local density functional theory can be successfully applied to the description of adsorption of nitrogen and argon on non-graphitized carbon black at their boiling points. The solid-fluid potential is determined from experimental adsorption isotherms and this potential was shown to decay faster compared to that predicted by the LJ equation. The developed method of application of NLDFT to amorphous solids and the determined experimentally solid-fluid potential can be further applied to modeling of adsorption in slit pores, which is important for characterization of activated carbons.

Acknowledgment. Support from the Australian Research Council is gratefully acknowledged.

REFERENCES

[1] E. P. Barrett, L. G. Joyner, P. P. Halenda, *J. Am. Chem. Soc.,* 1951, *73*, 373.
[2] M. Kruk, M. Jaroniec, A. Sayari, *Langmuir*, 1997, *13*, 6267.
[3] M. Kruk, V. Antochshuk, M. Jaroniec, A. Sayari, *J. Phys. Chem. B,* 1999, *103*, 10670.
[4] M. Kruk, M. Jaroniec, *Chem. Mater.* 2000, *12*, 222.
[5] E. A. Ustinov, D. D. Do, M. Jaroniec, "Pore Size Characterization of Mesoporous Materials by a Thermodynamic Approach: A Curvature-Dependent Solid-Fluid Potential" in "Nanoporous Materials IV" (A. Sayari, M. Jaroniec, Eds.), Elsevier, Amsterdam, 2005, pp. 663-672; Stud. Surface Sci. Catal. 155 (2005) 663-672.
[6] E. A. Ustinov, D. D. Do, M. Jaroniec, *Appl. Surf. Sci.* 2005 (Accepted - 1).
[7] A. E. Ustinov, D. D. Do, M. Jaroniec, *J. Phys. Chem., B.* 2005, *109,* 1947.
[8] B. V. Derjaguin, *Acta Physicochim. U.S.S.R.* 1940, *12*, 181.
[9] J C. P. Broekhoff, J. H. de Boer, *Journal of Catalysis*, 1967, *9*, 8, 15.
[10] J. C. P.Broekhoff, J. H.de Boer, *Journal of Catalysis*, 1968, *10*, 368, 377, 391.
[11] P. I. Ravikovitch, A. Neimark, V. *Studies in Surf. Sci. & Catal.,* 2000, *129,* 597.
[12] M. Jaroniec, M. Kruk, J. P. Olivier, *Langmuir*, 1999, *15,* 5410.
[13] N. A. Seaton, J. P. R. B. Walton, N. Quirke, *Carbon*, 1989, *27,* 853.
[14] C. Lastoskie, K. E. Gubbins, N. Quirke, *J. Phys. Chem*., 1993, *97,* 4786.
[15] C. Lastoskie, K. E. Gubbins, N. Quirke, *Langmuir,* 1993, *9,* 2693.
[16] P. Ravikovitch, A. Vishnyakov, R. Russo, A. Neimark, *Langmuir*, 2000, *16,* 2311.
[17] V. A. Bakaev, *J. Chem. Phys.* 1995, *102,* 1398.
[18] M. Kruk, M. Jaroniec, Yu. Bereznitski, *J. Colloid Interface Sci.,* 1996, *182,* 282.
[19] M. Kruk, M. Jaroniec, K. P. Gadkaree, *J. Colloid Interface Sci.,* 1997, *192,* 250.
[20] M. Kruk, Z. Li, M. Jaroniec, W. R. Betz, *Langmuir*, 1999, *15,* 1435.
[21] L. Gardner, M. Kruk, M. Jaroniec, *J. Phys. Chem., B,* 2001, *105,* 12516.
[22] P. I. Ravikovitch, A. Vishnyakov, A. V. Neimark, *Phys. Rev. E,* 2001, *64,* 011602.
[23] A. V. Neimark, P. I. Ravikovitch, *Microporous and Mesoporous Materials,* 2001, *44-45,* 697.
[24] E. A. Ustinov, D. D. Do, M. Jaroniec, *Appl. Surf. Sci.,* 2005 (Accepted - 2).
[25] P. Tarazona, *Phys. Rev. A,* 1985, *31,* 2672.
[26] P. Tarazona, U. M. B. Marconi, R. Evans, *Mol. Phys.,* 1987, *60,* 573.
[27] N. F. Carnahan, K. E. Starling, *J. Chem. Phys.,* 1969, *51,* 635.

[28] J. D. Weeks, D. Chandler, H. C. Andersen, *J. Chem. Phys.,* 1971, *54,* 5237.
[29] W. A. Steele, *Surf. Sci.,* 1973, *36,* 317.
[30] A. N. Tikhonov, *Dokl. Akad. Nauk SSSR*, 1943, *39*, 195.
[31] A. N. Tikhonov, *Dokl. Akad. Nauk SSSR*, 1963, *153*, 49.
[32] A. V. Neimark, P. I. Ravikovitch, M. Grün, F. Schüth, K. K. Unger, *J. Colloid Interface Sci.*, 1998, *207*, 159.
[33] E. A. Ustinov, D. D. Do, *Particle & Particle Systems Characterization,* 2004, *21,* 161.
[34] J. P. Olivier, *J. Porous Materials,* 1995, *2,* 9.